

Entrance channel cluster folding potentials for knockout reactions

Arun K. Jain* and B. N. Joshi†

Nuclear Physics Division, Bhabha Atomic Research Center, Mumbai-400 085, India

(Received 4 December 2007; revised manuscript received 23 January 2008; published 28 February 2008)

The entrance channel optical potentials for $(\alpha, 2\alpha)$ reactions are calculated using single folding models. These are found to be much different from the conventional entrance channel potentials and use of these folded entrance channel optical potentials significantly change the absolute cross sections. Small reductions in the entrance channel potentials are found to increase the peak to dip cross section ratios drastically for the knockout of α -clusters bound in the $\ell = 1$ state.

DOI: [10.1103/PhysRevC.77.027601](https://doi.org/10.1103/PhysRevC.77.027601)

PACS number(s): 24.50.+g, 24.10.Eq

There exist large anomalies in the DWIA analyses of the $(\alpha, 2\alpha)$ knockout reactions. Such anomalies presented orders of magnitude large α -cluster spectroscopic factors while using commonly accepted optical potentials and bound cluster wave functions [1–4]. Not only in $(\alpha, 2\alpha)$ reactions but in $(\alpha, \alpha^3\text{He})$, $(\alpha, \alpha t)$, and $(\alpha, \alpha d)$ reactions [5,6] also such large anomalies are seen. It was shown that the large discrepancy in the extracted spectroscopic factor at 140 MeV [7] (when a realistic value for the bound-state radius is employed) is not observed at 200 MeV [8,9]. Time to time various approximations which were made in the DWIA analyses were checked and were suitably modified [7]. These modifications accounted for only small variation in the results [7]. For example, off-shell effects were able to account for only up to a factor of two [10], the three-body final state coupling could account for only a few percent [11], and the discrete and continuous ambiguities in the final state optical potentials could account for factors of ~ 15 at the most [1]. These corrections still leave a large gap to be accounted for [1].

There exist some uncertainties about the entrance channel distorting potentials. The entrance channel potential is strictly the potential for the scattering of the incident particle from the residual nucleus which is to be averaged over the volume of the target nucleus [7]. Such a potential is not obtainable from any realistic experiment, therefore most of the DWIA calculations use potentials which reproduce the scattering data on the target nucleus, A but with a scaling down factor [7] equal to the ratio of the mass numbers of the residual nucleus, B and the target nucleus, $\frac{B}{A} V_{aA}$. This procedure had been adopted in almost all the cluster knockout DWIA calculations and had been found to be satisfactory as no significant shape changes in the DWIA results were witnessed even if the entrance channel potentials are changed substantially. However it can be seen that most of these studies were centered around the results where the clusters are bound in the $\ell = 0$ orbit. In the present work it is observed that with significant changes in the entrance channel optical potentials there are insignificant shape changes of the $\ell = 0$ knockout distribution. On the other hand with similar change in the entrance channel optical potentials substantial changes are observed in the shape of the $\ell = 1$ knockout

distribution. The most significant change is observed near the dip around the zero recoil momentum position for the $\ell = 1$ knockout. This indicates the important role the entrance channel optical potentials play in the filling up of the dip near the zero recoil momentum position and hence the shape of the spectral distribution for $\ell = 1$ spectra.

In view of the influence of the entrance channel optical potential, $V_{\text{Ent}}(r)$ on the DWIA calculations near the zero recoil momentum position (for $\ell = 1$ distribution) we have evaluated the entrance channel optical potentials for α -knockout reactions using a folding procedure. Here the projectile-ejectile interaction has been completely neglected as it has been already taken into account by the knockout t -matrix element.

For the $A(a, ab)B$ knockout reaction in the single folding model the effective interaction of the incident particle, a with the target nucleus, A is calculated in terms of its interactions with the residual nucleus, B and the struck particle, b . These interactions are folded over the density distribution of the target, which we approximated by the square of the ground state intercluster radial wave function.

$$V_{aA}(\vec{r}_{aA}) = \int \left[t_{ab} \left(\vec{r}_{aA} - \frac{B}{A} \vec{R} \right) + t_{aB} \left(\vec{r}_{aA} + \frac{b}{A} \vec{R} \right) \right] \times \rho(R) d\vec{R}. \quad (1)$$

As the projectile-ejectile, a - b interaction is completely accounted to all orders by the corresponding knockout t -matrix it has been neglected while calculating the entrance channel distorting potential, $V_{\text{Ent}}(r)$ for the knockout reaction. The effective interaction between a and B , $t_{aB}(\vec{r}_{aB})$ may be approximated by the a - B optical potential, $V_{aB}(\vec{r}_{aB})$. Therefore

$$V_{\text{Ent}}(\vec{r}_{aA}) = \int V_{aB} \left(\vec{r}_{aA} + \frac{b}{A} \vec{R} \right) \rho(R) d\vec{R}. \quad (2)$$

For the evaluation of this integral use is made of the conventional technique of using the Fourier transform of $V_{aB}(\vec{r}_{aB} + \frac{b}{A} \vec{R})$. If here we have $v(\vec{k})$ as the Fourier transform of the $V_{aB}(\vec{r}_{aB})$ then,

$$V_{\text{Ent}}(\vec{r}_{aB}) = \int e^{-i\vec{k}\cdot\vec{r}_{aB}} v(\vec{k}) d\vec{k}. \quad (3)$$

* arunjain@barc.gov.in

† bnjoshi@barc.gov.in

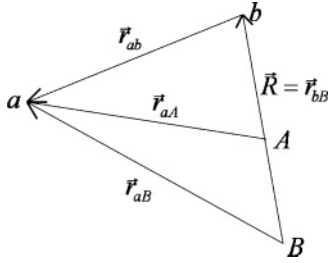


FIG. 1. Schematic vector diagram for the various coordinates used in the cluster folding model.

The variables \vec{r}_{aA} and \vec{R} are now easily separated in Eq. (2) to yield

$$V_{\text{Ent}}(\vec{r}_{aA}) = \iint e^{-i\frac{b}{A}\vec{k}\cdot\vec{R}} \rho(R) d\vec{R} e^{-i\vec{k}\cdot\vec{r}_{aA}} v(\vec{k}) d\vec{k}. \quad (4)$$

Now assuming a spherical density $\rho(R)$ (to be taken as $|\phi_{bB}(R)|^2$) one gets the entrance channel potential $V_{\text{Ent}}(r_{aA})$,

$$V_{\text{Ent}}(r_{aA}) = (4\pi)^2 \int \rho(R) F(r_{aA}, R) R^2 dR, \quad (5)$$

where

$$F(r_{aA}, R) = \int J_0\left(\frac{m_b}{m_A} kR\right) J_0(kr_{aA}) v(k) k^2 dk. \quad (6)$$

Using Eqs. (5) and (6) we have evaluated the entrance channel optical potentials for ${}^7\text{Li}(\alpha, 2\alpha){}^3\text{H}$, ${}^{12}\text{C}(\alpha, 2\alpha){}^8\text{Be}$, ${}^{16}\text{O}(\alpha, 2\alpha){}^{12}\text{C}$, and many other α -cluster knockout reactions at various energies. For the ${}^7\text{Li}(\alpha, 2\alpha){}^3\text{H}$ reaction the α - ${}^3\text{H}$ optical potentials of Warner *et al.* [3] have been used to obtain the effective entrance channel optical potentials by employing the 3.54 fm rms radius α - ${}^3\text{H}$ bound intercluster wave function for calculating $\rho(R)$ of ${}^7\text{Li}$. For the evaluation of the entrance channel optical potentials for the ${}^{12}\text{C}(\alpha, 2\alpha){}^8\text{Be}$ and ${}^{16}\text{O}(\alpha, 2\alpha){}^{12}\text{C}$ reactions the corresponding α - ${}^8\text{Be}$ and α - ${}^{12}\text{C}$ optical potentials are taken to be the same as in the exit channel which are then folded over the corresponding density $\rho(R)$. It is to be reminded that $\rho(R)$'s are obtained from the respective bound intercluster wave functions which were employed in the entrance channel bound state description. For the α - ${}^3\text{H}$ bound state description of ${}^7\text{Li}$ the 3.54 fm rms radius α - ${}^3\text{H}$ bound $\ell = 1$ intercluster wave function has been used. The 200 MeV ${}^{12}\text{C}(\alpha, 2\alpha){}^8\text{Be}$ reaction analysis uses the $1.23 \times 8^{\frac{1}{3}}$ radius Woods-Saxon potential to generate the $\ell = 0$ bound α - ${}^8\text{Be}$ wave function. The analyses of the 140 MeV ${}^{12}\text{C}(\alpha, 2\alpha){}^8\text{Be}$ and ${}^{16}\text{O}(\alpha, 2\alpha){}^{12}\text{C}$ reactions use the $2.52 \times 8^{\frac{1}{3}}$ fm and $2.52 \times 12^{\frac{1}{3}}$ fm radius Woods-Saxon potentials respectively to generate the $\ell = 0$ intercluster bound wave functions.

For different reactions the various entrance channel optical potentials are compared in Fig. 2. In this figure all the folded entrance channel potentials are seen to be much different from those obtained from either the $\frac{B}{A}V_{aA}$ criterion or the V_{aA} approximation. The folded imaginary potentials are seen to be deeper than the $\frac{B}{A}V_{aA}$ potentials. Both the real and imaginary folded potentials are more diffused than the $\frac{B}{A}V_{aA}$ potentials. However, the Wang *et al.* [1] potentials employed for the

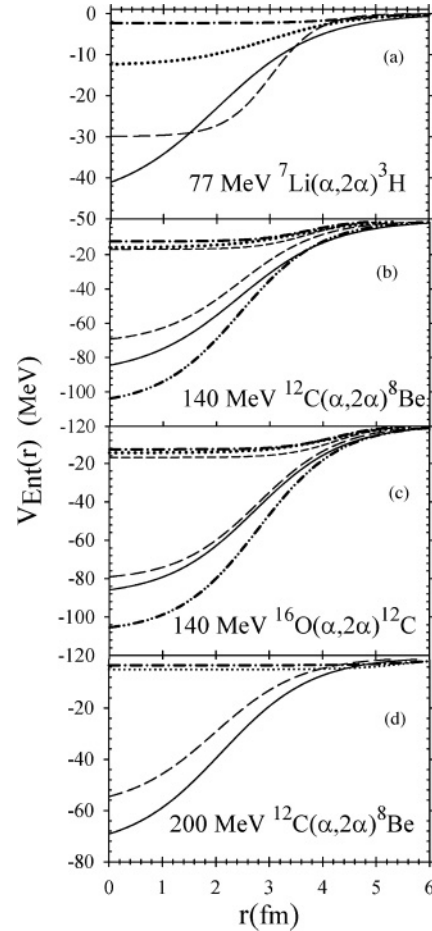


FIG. 2. Various entrance channel optical potentials, (—) real folded, (\dots) imaginary folded, (---) real $\frac{B}{A}V_{aA}$ prescription, and (-.-.-) imaginary $\frac{B}{A}V_{aA}$ prescription. The 140 MeV results used (-.-.-) real V_{aA} and (---) imaginary V_{aA} optical potentials. (a) is for 77 MeV ${}^7\text{Li}(\alpha, 2\alpha){}^3\text{H}$, (b) is for 140 MeV ${}^{12}\text{C}(\alpha, 2\alpha){}^8\text{Be}$, (c) is for 140 MeV ${}^{16}\text{O}(\alpha, 2\alpha){}^{12}\text{C}$, and (d) is for 200 MeV ${}^{12}\text{C}(\alpha, 2\alpha){}^8\text{Be}$ reactions.

140 MeV data analyses are deeper than even the folded potentials.

Using the entrance channel optical potentials of Fig. 2(a) along with the exit channel α - ${}^3\text{H}$ optical potentials from Warner *et al.* [3] the 77 MeV ${}^7\text{Li}(\alpha, 2\alpha){}^3\text{H}$ reaction cross sections were calculated in the conventional DWIA formalism. The folding model results are compared with the data as well as with the corresponding results obtained from the $\frac{B}{A}V_{aA}$ criterion in Fig. 3. In order to highlight various shape and magnitude changes as a result of changing the entrance channel potentials the DWIA calculations shown in this report are not normalized to the respective experimental data. It is seen that the two calculations agree reasonably well with each other in shape. However the folding model results are about a factor two smaller in absolute magnitude. In both the calculations however, the dip at the zero recoil momentum position can be seen to be still filled up in comparison to the experimental results. It can also be seen in Fig. 3 that when the entrance channel potential depths, both in the $\frac{B}{A}V_{aA}$ as well as from the folding criterion, are reduced by about 25% the peak to dip

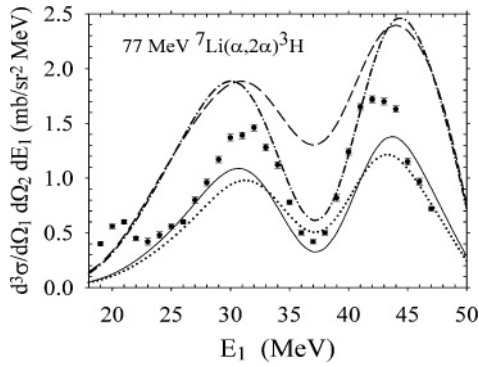


FIG. 3. The DWIA calculations using various entrance channel potentials, (---) Warner *et al.*, (-.-.-) 0.7 times Warner *et al.*, (.....) folded V_{AA} , and (—) 0.8 times folded V_{AA} compared with the 77 MeV ${}^7\text{Li}(\alpha, 2\alpha){}^3\text{H}$ reaction data.

ratio increases sharply. As there are only marginal changes in the peak cross section values the sharp change can be seen to arise mainly due to large relative changes in the dip cross section values. The surprising part is that this ratio is almost unchanged while going from folding to $\frac{B}{A} V_{AA}$ criterion. Although it is not the main issue of this report but it is to be remarked that for ${}^7\text{Li}$ the theoretical α - t spectroscopic factor, $S_\alpha \approx 1.15$ and a multiplication of the solid curve in Fig. 3 by this S_α will result in very good agreement with the data. These findings are not unique to the 77 MeV ${}^7\text{Li}(\alpha, 2\alpha){}^3\text{H}$ reaction alone as the 119 MeV ${}^7\text{Li}(\alpha, 2\alpha){}^3\text{H}$ reaction analysis seen in Fig. 4 also shows similar behavior. It is to be conceived that the filling of the dip is due to a delicate balance of the interference of the entrance and exit channel distorted waves which produce the dip in the $\ell \neq 0$ spectra at the zero recoil momentum position.

Why is the folding model potential reduced further for fitting the data? The reason may be in the use of free a - B optical potential, V_{aB} while it should actually be a reduced effective potential t_{aB} . It is also conceivable that the use of an effective potential t_{aB} will provide optical potential smaller in magnitude in comparison to the one obtained from the free aB scattering due to the restricted phase space available to the scattering of a on bound B . It may also be partly due to the density, $\rho(R)$ being taken as $|\Phi_{aB}(R)|^2$ while it should be an average over the other configurations weighted with respective spectroscopic factors. From the energy dependence of the

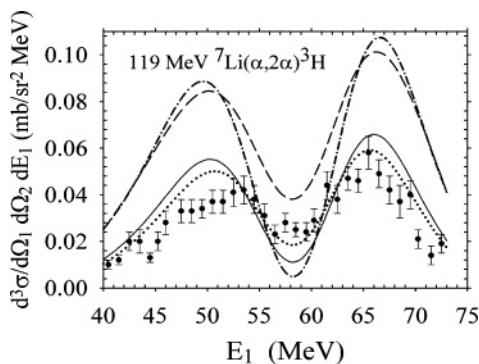


FIG. 4. Same as Fig. 3 but for 119 MeV ${}^7\text{Li}(\alpha, 2\alpha){}^3\text{H}$ data.

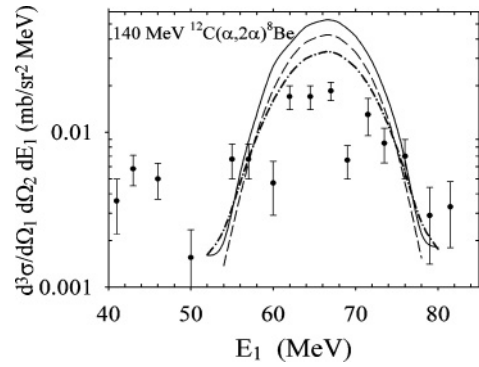


FIG. 5. The DWIA calculations using various entrance channel potentials, (—) folded V_{aA} , (---) $\frac{B}{A}$ times Wang *et al.* V_{aA} (-.-.-) Wang *et al.* V_{aA} for the 140 MeV ${}^{12}\text{C}(\alpha, 2\alpha){}^8\text{Be}$ reaction.

(77 MeV, 99 MeV, and 119 MeV) ${}^7\text{Li}(\alpha, 2\alpha){}^3\text{H}$ reaction data, however, it is seen that the dip is more filled up in the higher energy data. This indicates that at higher energies the influence of the cluster separation energy on the t_{aB} is reduced in comparison to that at lower energies. The overall reduction in the cluster knockout cross sections using the folded potentials in the entrance channel seems to be arising from the larger strength of the imaginary component of the folded potentials.

A comparison of the DWIA predictions using these entrance channel potentials for the $\ell = 0(\alpha, 2\alpha)$ reactions is shown in Figs. 5–7. In order to highlight the change in magnitude the DWIA results again have not been normalized to the data. It is seen in Figs. 5 and 6 for the 140 MeV ${}^{12}\text{C}(\alpha, 2\alpha){}^8\text{Be}$ and ${}^{16}\text{O}(\alpha, 2\alpha){}^{12}\text{C}$ reactions respectively that the entrance channel potentials do not change the shape vary significantly while the magnitudes vary by a factor of up to two. This will thus affect the α -spectroscopic factor within a factor of two only. The results of the 200 MeV ${}^{12}\text{C}(\alpha, 2\alpha){}^8\text{Be}$ reaction again show a similar trend that the DWIA calculations provide an α -spectroscopic factor within a factor of two, but the shape is hardly affected by the use of different entrance channel optical potentials. From these $\ell = 0$ α -knockout results one can infer that as a result of a variation of the entrance channel optical potentials the calculated absolute cross sections change within a factor of two while there is no appreciable change in the shape of the spectra. On the other hand the DWIA predictions for the $\ell = 1$ α -knockout using various entrance channel optical

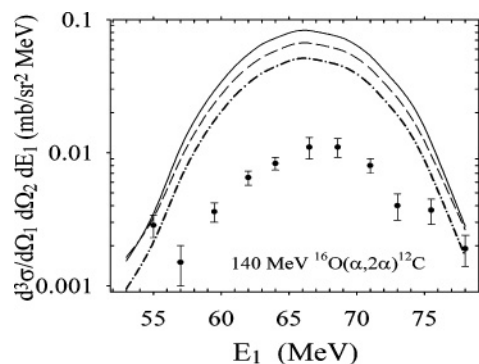


FIG. 6. Same as Fig. 5 but for 140 MeV ${}^{16}\text{O}(\alpha, 2\alpha){}^{12}\text{C}$ reaction.

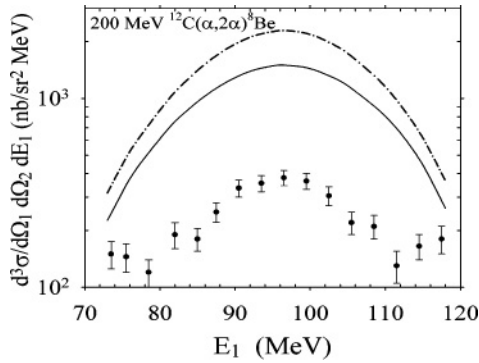


FIG. 7. The DWIA calculations using various entrance channel potentials, (—) folded V_{aA} , (---) Steyn *et al.* V_{aA} for the 200 MeV $^{12}\text{C}(\alpha, 2\alpha)^8\text{Be}$ reaction.

potential prescription change both magnitude as well as shape of the spectra.

It can therefore be concluded that the discrepancy in the peak to dip cross section ratios in the conventional DWIA predictions of $\ell = 1$ spectra is mainly due to the uncertainties in the choice of the entrance channel potentials. In fact the entrance channel potentials can be obtained through a

consistent procedure of folding the exit channel potentials over the density distribution obtained from the intercluster wave function. To be more specific we found that in the case of cluster knockout reactions on light-medium mass nuclei the depths of the folded potentials are much different from the $\frac{B}{A}V_{aA}$ potentials. The use of folded potentials in the entrance channel are seen to change the DWIA predictions, by a factor of \sim two at the most, in comparison to those obtained using the $\frac{B}{A}V_{aA}$ criterion. Whereas the folding model entrance channel optical potentials are expected to be more consistent for the DWIA analyses of the the α -cluster knockout data (especially for the $\ell = 1$ α -knockout) the use of the cluster folding potentials appear to be more consistent and aesthetically satisfying for other knockout reactions also.

The authors would like to thank the Department of Science and Technology, Government of India for supporting this work through Project Grant No. SR/S2/HER-09/2004. Our thanks are also to the Bhabha Atomic Research Centre, Mumbai for providing the necessary infrastructure and logistics support. Our special thanks are to Dr. V. C. Sahni, Dr. S. Kailas, and Dr. R. K. Choudhury for their keen interest in this work and encouragement.

-
- [1] C. W. Wang, N. S. Chant, P. G. Roos, A. Nadasen, T. A. Carey *et al.*, Phys. Rev. C **21**, 1705 (1980).
 [2] N. S. Chant, P. G. Roos, and C. W. Wang, Phys. Rev. C **17**, 8 (1978).
 [3] R. E. Warner, A. Okihana, M. Fujiwara, N. Matsuoka, S. Kakigi, S. Hayashi, K. Fukunaga, J. Kasagi, M. Tosaki *et al.*, Phys. Rev. C **45**, 2328 (1992).
 [4] Arun K. Jain and S. Mythili, Phys. Rev. C **53**, 508 (1996).
 [5] C. Samanta, N. S. Chant, P. G. Roos, A. Nadasen, A. A. Cowley *et al.*, Phys. Rev. C **26**, 1379 (1982).
 [6] C. Samanta, N. S. Chant, P. G. Roos, A. Nadasen, A. A. Cowley *et al.*, Phys. Rev. C **35**, 333 (1987).
 [7] N. S. Chant and P. G. Roos, Phys. Rev. C **15**, 57 (1977).
 [8] A. A. Cowley, G. F. Steyn, S. V. Fortsch, J. J. Lawrie, J. V. Pilcher, F. D. Smit, D. M. Whittal *et al.*, Phys. Rev. C **50**, 2449 (1994).
 [9] G. F. Steyn, S. V. Fortsch, A. A. Cowley, J. J. Lawrie, G. J. Arendse, G. C. Hillhouse, J. V. Pilcher, F. D. Smit, R. Neveling *et al.*, Phys. Rev. C **59**, 2097 (1999).
 [10] N. R. Sharma and B. K. Jain, Nucl. Phys. **A377**, 201 (1982).
 [11] Arun K. Jain, Phys. Rev. C **45**, 2387 (1992).